DEUTSCHES ELEKTRONEN-SYNCHROTRON DESY

DESY 79/51
August 1979

THE DYNAMICS OF THE REACTION $\gamma p \rightarrow p\bar{p}p$ AT ENERGIES BETWEEN 4.7 AND 6.5 GeV

by

J. Bodenkamp, D. C. Fries, A. Markou, E. Seitz

Institut für Kernphysik des Kernforschungszentrums
und
Institut für Experimentelle Kernphysik der Universität Karlsruhe

H. J. Behrend, W. P. Hesse, T. Miyachi,
W. A. McNeely Jr., V. Schröder

Deutsches Elektronen-Synchrotron DESY, Hamburg

NOTKESTRASSE 85 · 2 HAMBURG 52

Contribution to "1979 International Symposium on Lepton and Photon Interactions at High Energies", Fermilab, August 1979.

DESY 79/51
August 1979

The dynamics of the reaction $\gamma p \rightarrow p\bar{p}p$ at energies between 4.7 and 6.5 GeV.

J. Bodenkamp, D. C. Fries, A. Markou, E. Seitz

Institut für Kernphysik des Kernforschungszentrums und Institut für Experimentelle Kernphysik der Universität, Karlsruhe

H. J. Behrend, W. P. Hesse *, T. Miyachi **, W. A. Mc Neely Jr. ***, V. Schröder

Deutsches Elektronensynchrotron DESY, Hamburg

Abstract

In a photoproduction experiment at DESY the reaction $\gamma p \rightarrow p\bar{p}p$ has been investigated. The basic dynamics by which this reaction proceeds has been identified.

* Dep. of Physics, Randolph-Macon College, Ashland, Va. 23005, USA

** Institute for Nuclear Study, Univ. of Tokyo, Tanashi City, Tokyo 188, Japan

*** Boeing Computer Services, Seattle, Washington 91868, USA

1) Introduction

An experiment has been performed at the 7 GeV Electron Synchrotron, DESY, in which the photoproduction of proton antiproton pairs from hydrogen has been studied.
We report in this paper on first results of the analysis of the reaction

(1) $\gamma p \rightarrow p\bar{p}p$

in particular on our identification of the gross dynamical features by which reaction (1) proceeds.

The experimental evidence on reaction (1) which has so far been collected is very scarce [1,2]. The interest in this reaction however, is considerable, since (1) constitutes an alternative approach to solve the riddle of low energy $p\bar{p}$ interactions. Viewed on the basis of a quark picture the proton antiproton system poses a well known problem: Duality would predict that $p\bar{p}$ form a 4 quark system in flavors u, d and $\bar{u}$, $\bar{d}$:

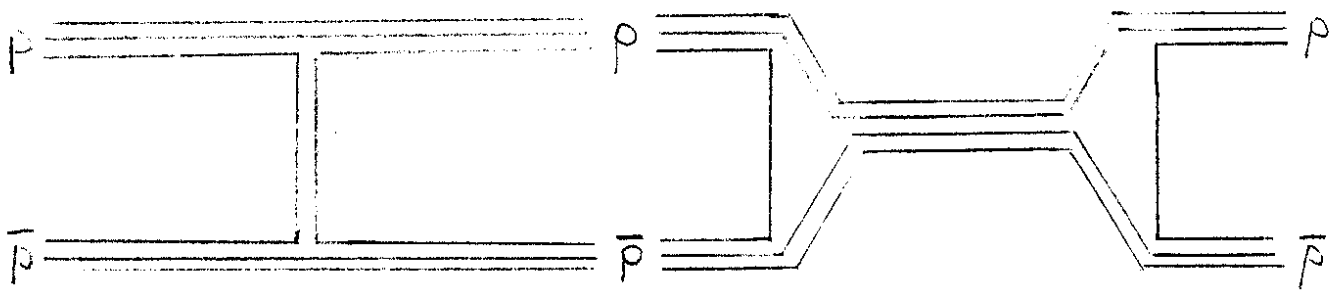

Mesonic states of the type $qq\bar{q}\bar{q}$ or of the type diquark antidiquark (qq) $(\bar{q}\bar{q})$, which are expected to exist [3], however have not been identified with certainty, so far. Special implications arise in photoproduction of proton antiproton pairs. After a description of the apparatus an analysis of the main dynamical features of the $p\bar{p}$ photoproduction, based on our experimental data is presented.

2) Experimental procedures and Data reduction

The experimental set up is shown in Fig. 1 [4]. Photons with energies between 4.5 and 6.2 GeV being marked in a tagging system impinge on a target of 50 cm liquid hydrogen. Charged tracks from the target are recorded by two prop-chambers inside and 8 sparkchambers downstream of a large bending magnet. The tracks crossing 3 hodoscope planes of scintillation counters trigger either the counters of a time-of-flight (TOF) system or traverse a threshold Cerenkov counter, which discriminates against fast pions and electrons.

The photon beam and a fraction of the e^+e^- pairs have been blocked out using a lead beam stopper inside of the magnet. The event trigger required at least two tracks crossing the hodoscope planes and one particle triggering the TOF counters. Track identifying, fast decision making electronic logic has been used.

Totally 1.5×10^6 triggers have been collected. Selecting a subsample for which a unique TOF information existed, we observe, by computing the particle mass from the TOF information, a strong signal at the proton mass for positively charged tracks (Fig. 2). The antiproton mass signal in the raw data sample is, however, marginal, due to the small production cross section of the reaction (1). After the geometric reconstruction the events were subjected to a one constraint kinematic fit for the hypotheses of the main competing reactions:

$\gamma p \rightarrow p\pi^+\pi^-$, $\gamma p \rightarrow pk^+k^-$, $\gamma p \rightarrow pp\bar{p}$

Accepting events which yield a fit with a good probability only for the $p\bar{p}$-hypothesis, the distribution of the TOF-computed masses (for negative tracks) showed an accumulation around the proton mass. This sample of about 65 events was identified as events due to reaction (1).

We made two tests in order to cross check our selection procedure:

a) selecting events due to the hypothesis $\gamma p \rightarrow p\pi^+\pi^-$ in an analogous manner, we obtain a clean ρ^0 signal in the invariant $\pi^+\pi^-$ mass (Fig. 3)

b) varying the proton and antiproton rest masses in steps around the true particle masses and plotting the number of events, accepted with the above procedure, versus the particle mass, the number of accepted events shows a clear maximum at the true proton mass (Fig. 4).

3) Analysis and Discussion

The evaluation of the invariant $p\bar{p}$ mass from experimental data involves for reaction (1) a principle ambiguity concerning which of the protons has interacted with the antiproton or recoiled from the $p\bar{p}$ system in the overall center-of-mass frame (CM). If reaction (1) proceeds basically via a peripheral t channel exchange [5] :

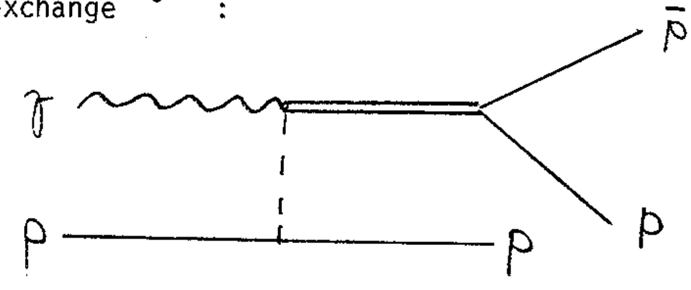

one would expect that the distribution of the observed proton momenta shows two accumulations, one at low (recoil) and one at higher momentum.

Our data exhibit indeed two separate accumulations in the proton momentum spectrum at 1 resp. 2.5 GeV (Fig. 5 b).
The $| t - t_{min} |$ distribution, where t is the four momentum transfer squared to the $p\bar{p}$ system (considering the slow proton as recoiling), is however flat up to 6 $(\frac{GeV}{c})^2$ and indicates in no way a peripheral process (Fig. 6). Furthermore the distribution of the antiproton momentum shows no similarity with the momentum distribution of the 'fast' proton, which could be expected if the peripheral process applies.
A Monte Carlo simulation of the t channel exchange dynamics, taking in account, in a detailed way, the properties of the experimental apparatus, the trigger conditions and the applied cuts, yield data, which were compared to the observed distributions (after suitable normalisation).
This comparison is shown in Figs. 7 a, b. The inconsistancy of the peripheral dynamics with the data is seen most clearly in the antiproton momentum distribution. Also the spectrum of the recoil proton is ill matched to the corresponding spectrum of the simulated events.

As an alternative we studied the possibility, that the basic dynamical features of reaction (1) can be described by a nucleon or u channel exchange diagram:

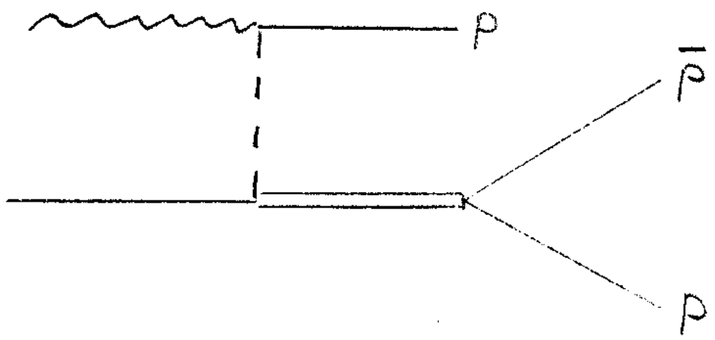

That is to say, we consider a process where the virtual antiproton and the target proton form an interacting system, being produced in backward direction in the CM frame.
We simulated Monte Carlo data for the $\bar{u}$ channel dynamics assuming an exponential $| u - u_{min} |$ distribution with a slope parameter of - 6.0 $(\frac{GeV}{c})^{-2}$, an isotropic angular decay distribution of the $\bar{p}$ in the $p\bar{p}$ rest frame and a distribution of the $p\bar{p}$ invariant mass, which corresponded roughly to the observed one. In Fig. 8 we compare the simulated and the experimental distributions.

We find an excellent agreement for the antiproton momentum spectrum and for both, the low and high momentum part of the proton momentum spectrum. The experimental $| u - u_{min} |$ distribution shows the exponential sloping (Fig. 6 a), assumed for the simulated events. In addition, by optimizing the slope parameters and the parameters of the $p\bar{p}$ decay distribution this model describes also reasonably well the relative strength of the observed antiproton, recoil and fast proton signals.

On the basis of this model we can now evaluate the invariant $p\bar{p}$ mass in an unambignous way. The distribution of $m_{p\bar{p}}$, not corrected for acceptance losses, is shown in Fig. 9. On the basis of our statistics it cannot be decided whether this distribution contains any resonant structures. A final analysis concerning acceptance corrected spectra and cross sections is in preparation.

Acknowledgements

We like to thank the DESY machine staff and Hallendienst and in particular our technician Mr. W. Burmester for their help and support in preparing and running the experiment.

The Karlsruhe group gratefully acknowledges the hospitality of DESY and the financial support of the Bundesministerium für Forschung und Technologie and of the Kernforschungszentrum Karlsruhe.

References and Footnotes

1) H. M. Bingham et al. Phys. Rev. D8 (1973), 1277.

2) D. Aston et al. XIX Intern. Conf. on High Energy Physics Tokyo 1978.

3) See for example:
J. L. Rosner Phys. Rev. Lett. 21 (1968), 950
Chan Hong Mo, H. Høgaasen, Phys. Lett. 72B (1977), 121
R. L. Jaffe, Phys. Rev. D17 (1978), 1444.

4) The experimental apparatus is a modified version of the one used in a previous experiment:
H. J. Behrend et al. Nucl. Phys. B144 (1978), 22
see also: A. Markou Dissertation Karlsruhe 1979.

5) This case has been discussed by
A. Wattenberg et al. proceedings of the Syracuse Symposium on $N\bar{N}$ Interactions, 1975.

6) Similar diagrams have been discussed in connection with hadronic processes. See R. L. Jaffe reference 3).

Figures

1) Experimental apparatus.

2) Masses of positively charge particles computed from TOF information.

3) Invariant $\pi^+\pi^-$ mass of events selected through a kinematic fit.

4) Number of accepted events, selected by a kinematic fit of the hypothesis $\gamma p \to pXX$ and TOF versus the particle mass X.

5 a, b) Experimental momentum spectrum of antiprotons and protons of the final sample selected for (1).

6) a) $| U - U_{min} |$ distribution using the 'slow' protons
b) $| t - t_{min} |$ distribution using the 'fast' protons.

7) Comparison of events simulated due to a pheripheral diagram with experimental spectra.

8) Comparison of events simulated due to a nucleon exchange diagram with experimental momentum spectra.

9) $p\bar{p}$ invariant mass distribution (not corrected for losses).

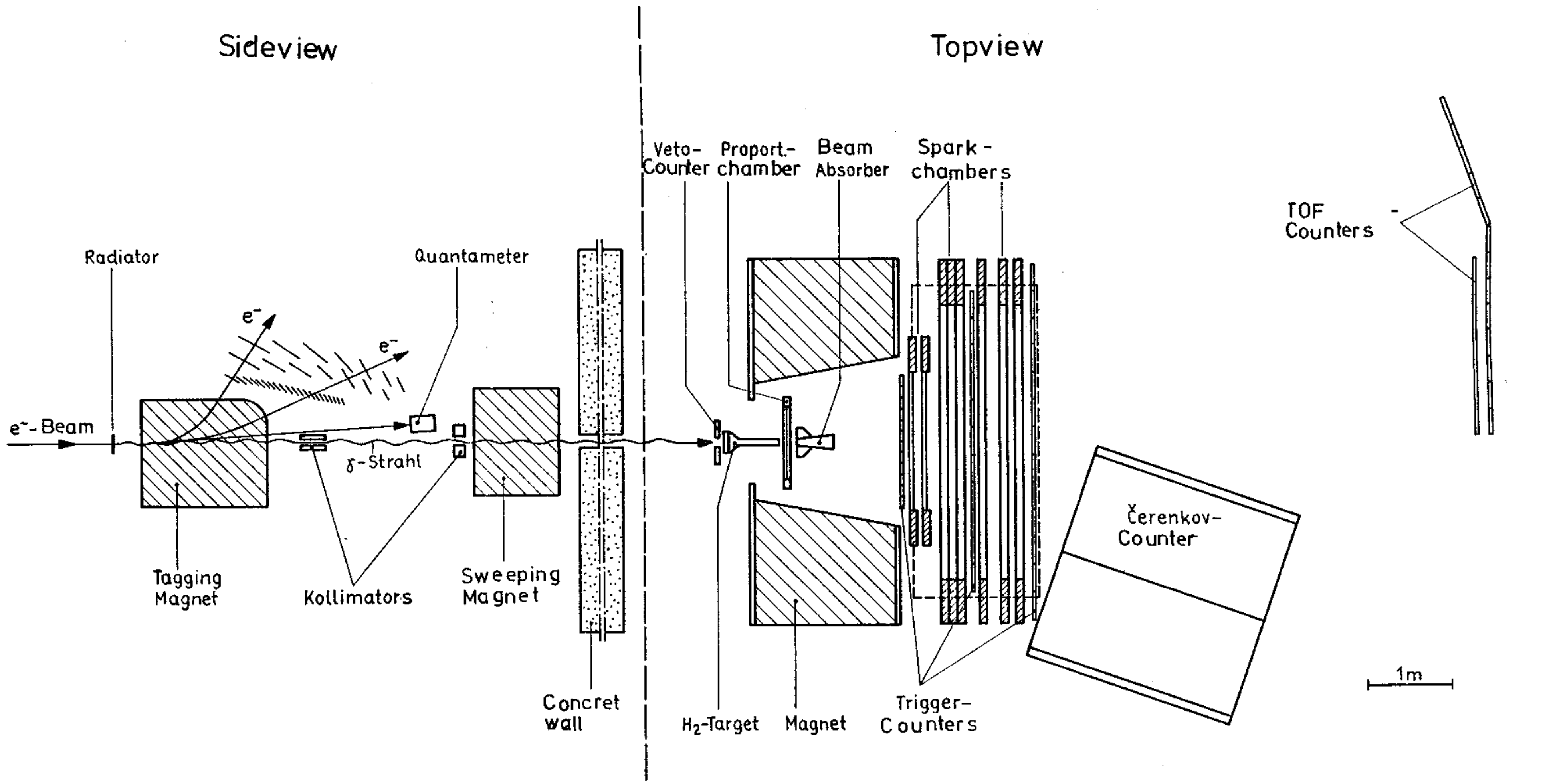
Sideview
Topview
e⁻-Beam
Radiator
Tagging Magnet
e⁻
e⁻
Quantameter
γ-Strahl
Kollimators
Sweeping Magnet
Concret wall
Veto-Counter
Proport.-chamber
Beam Absorber
Spark-chambers
TOF Counters
H₂-Target
Magnet
Trigger-Counters
Čerenkov-Counter
1m

Fig. 1

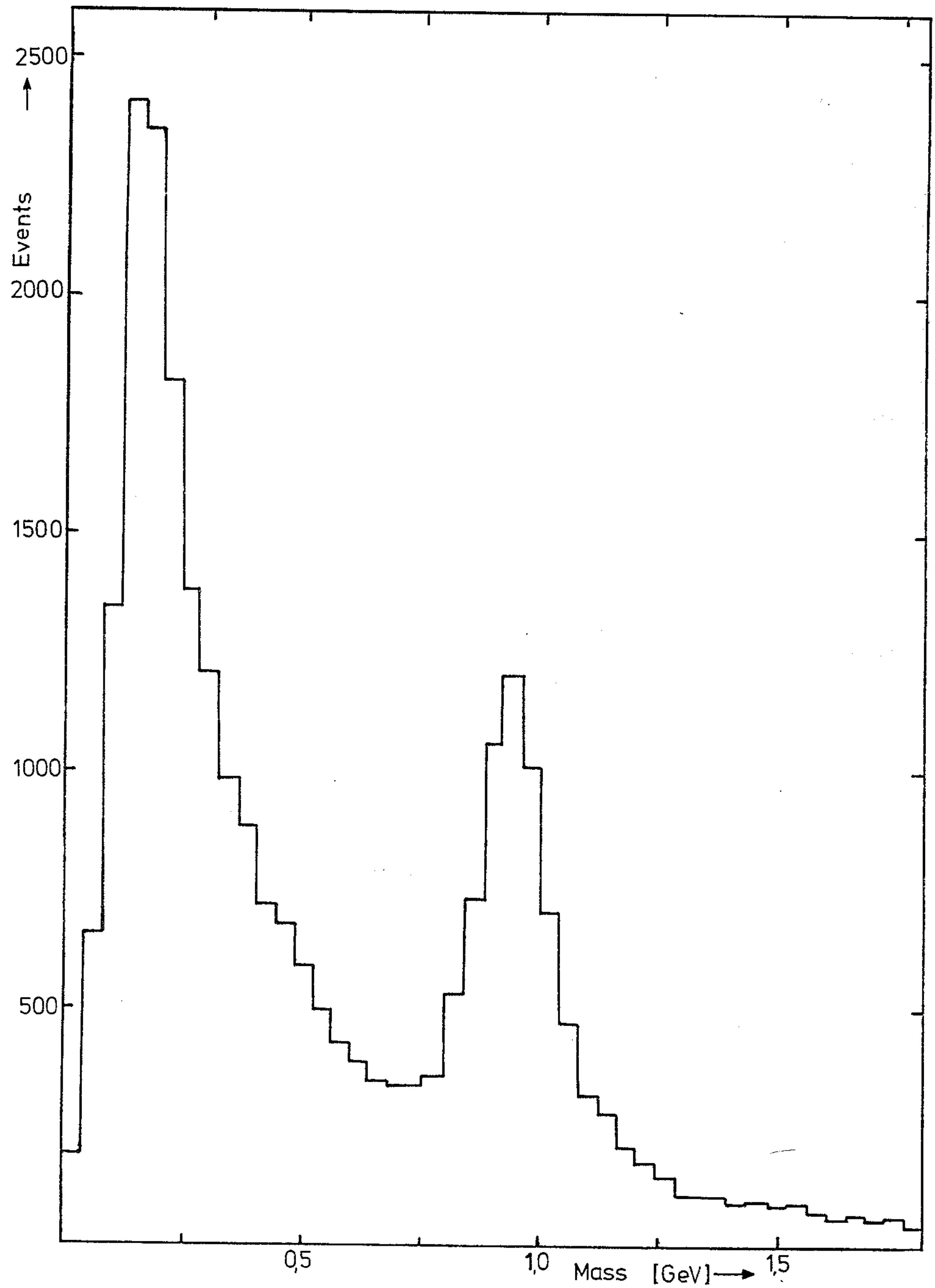

Fig. 2

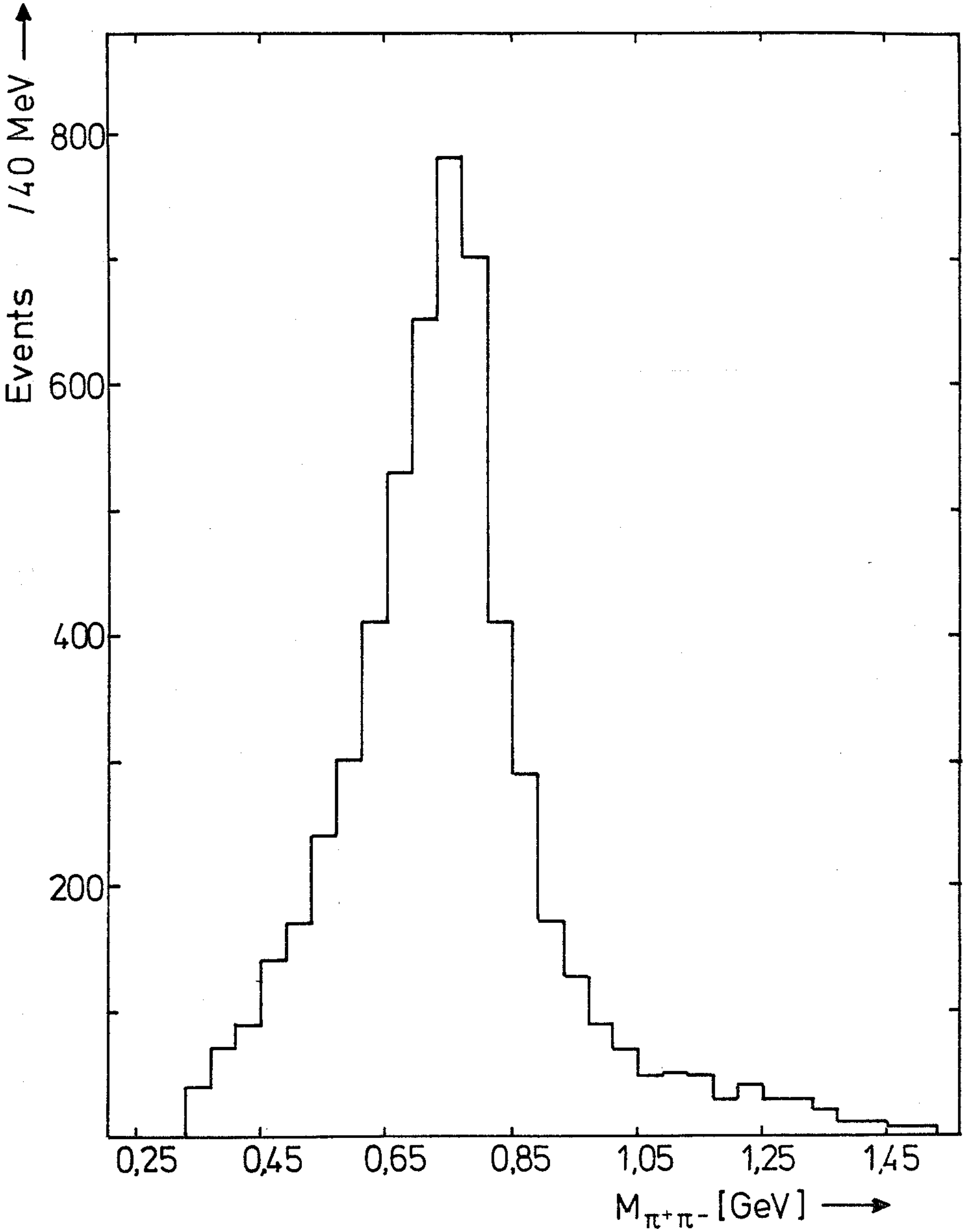

Events /40 MeV
800
600
400
200
0,25
0,45
0,65
0,85
1,05
1,25
1,45
$M_{\pi^+\pi^-}$ [GeV]

Fig. 3

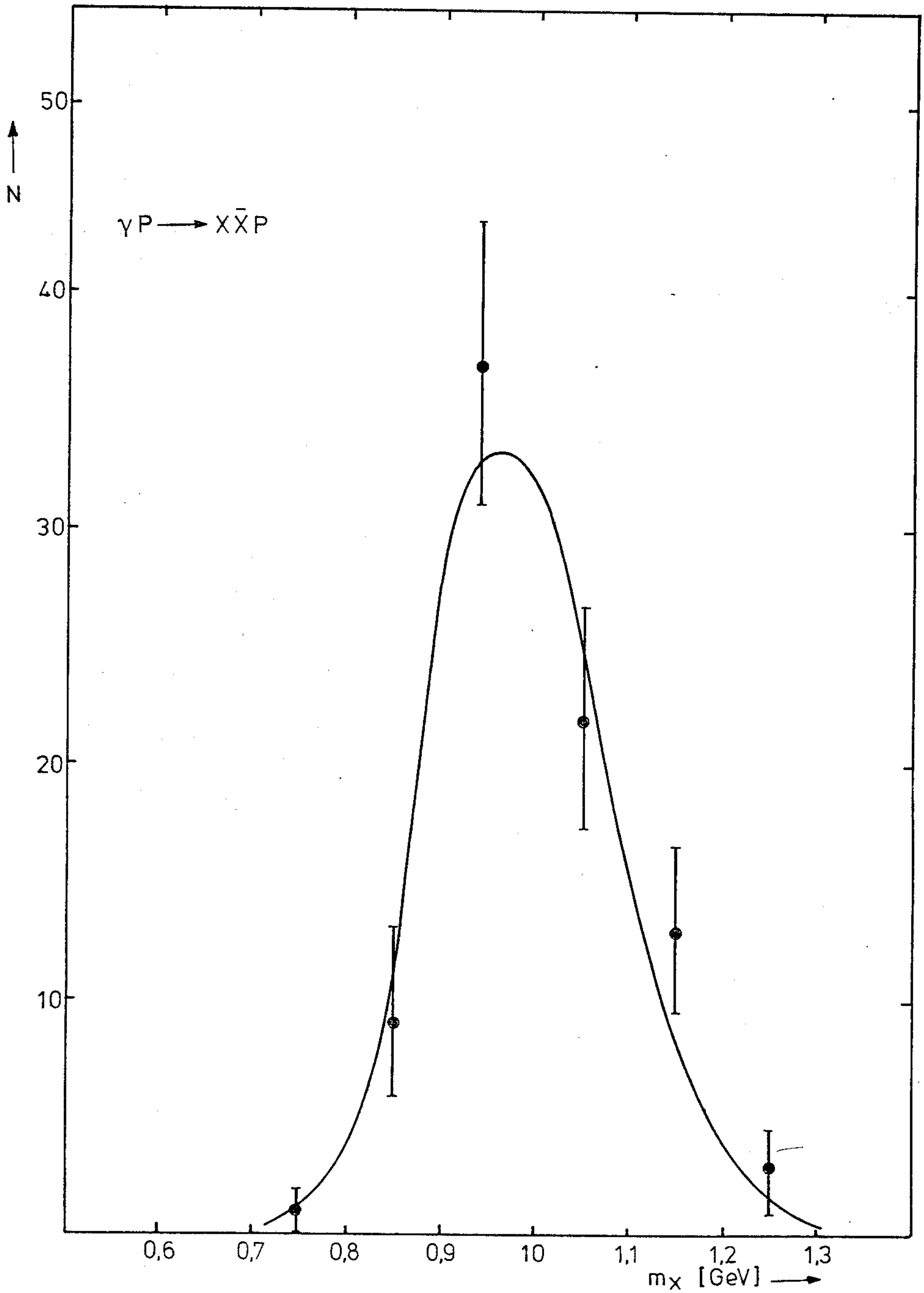

Fig. 4

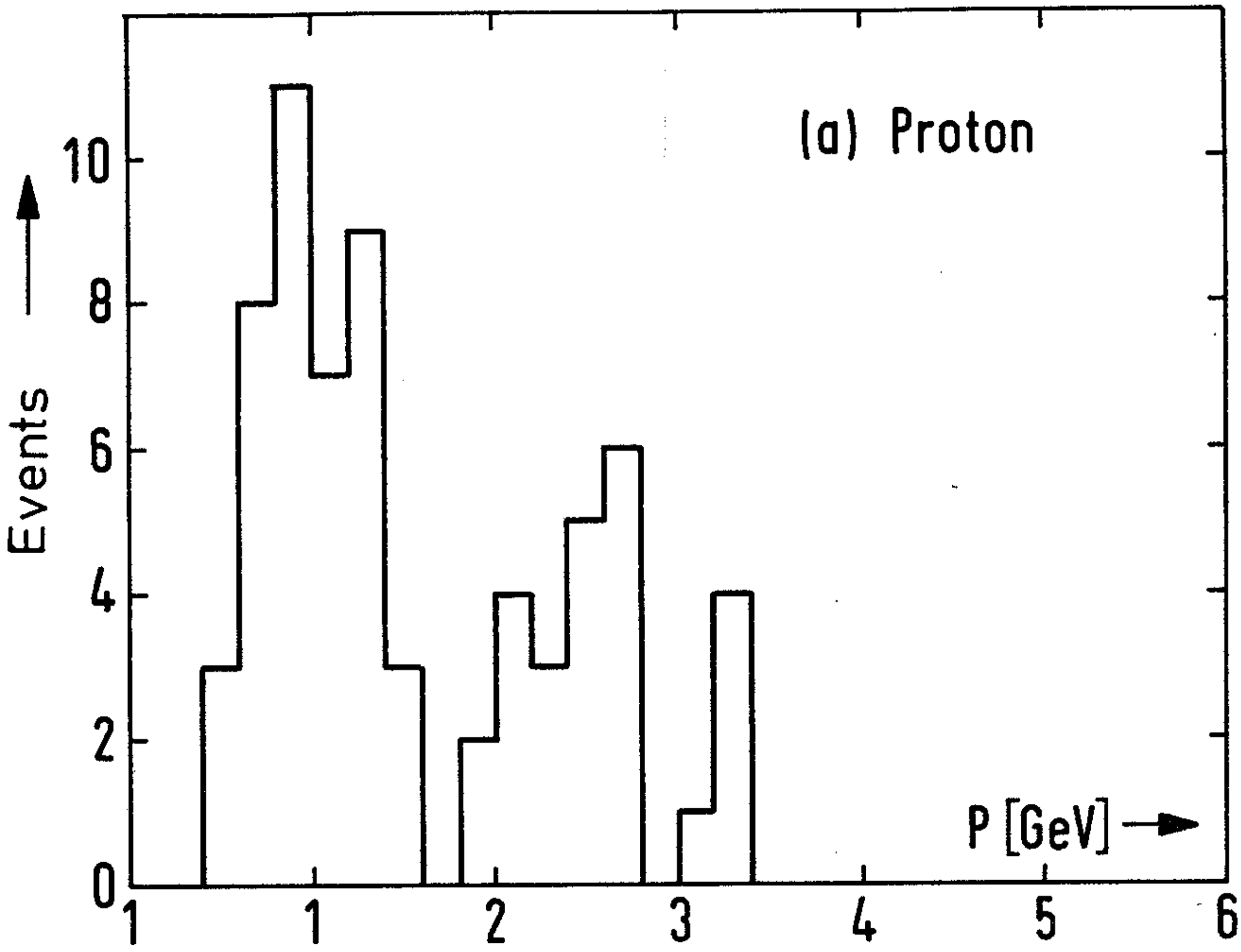

(a) Proton
Events
P [GeV]
0
2
4
6
8
10
1
1
2
3
4
5
6

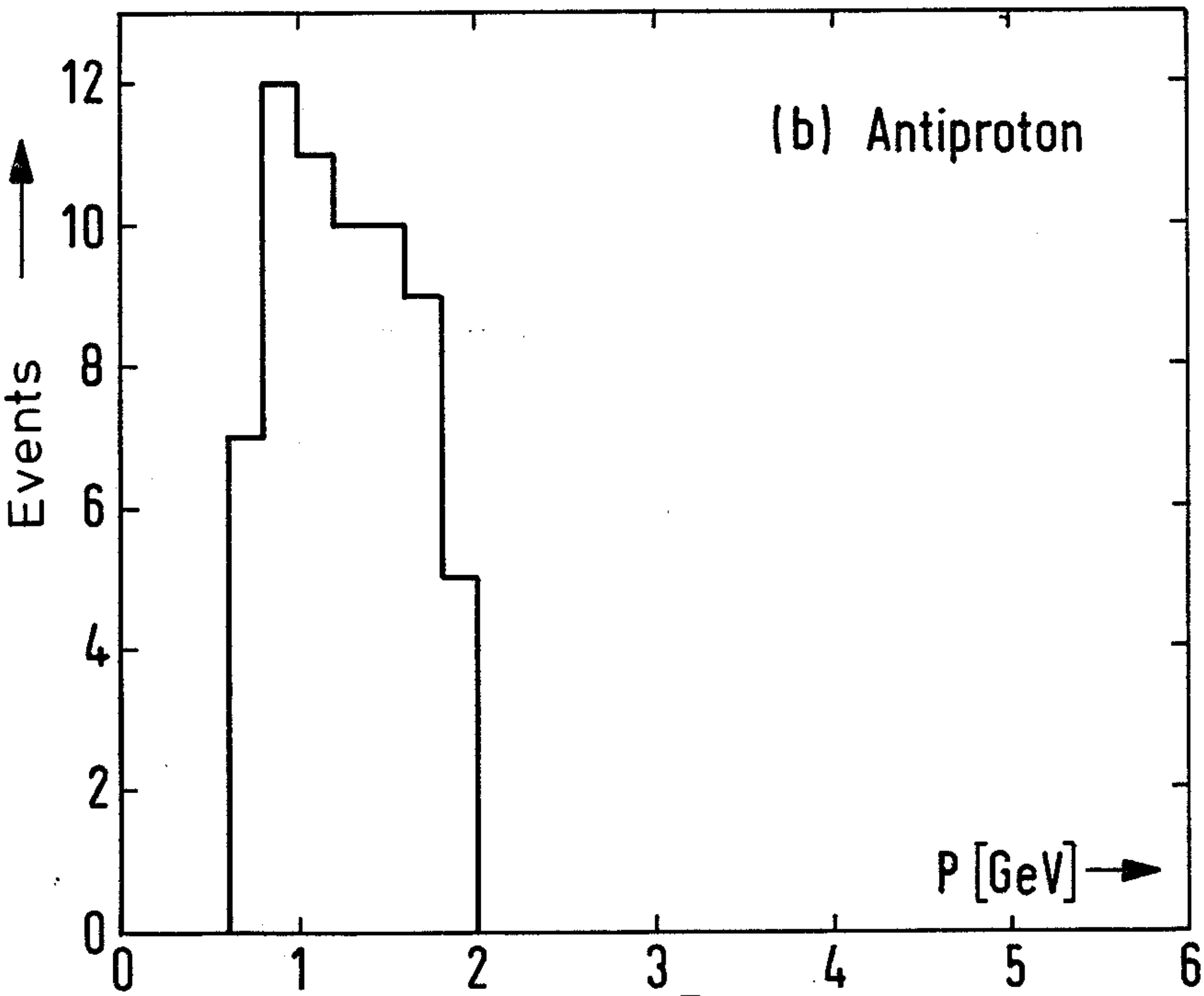

(b) Antiproton
Events
P [GeV]
0
2
4
6
8
10
12
0
1
2
3
4
5
6

Fig. 5

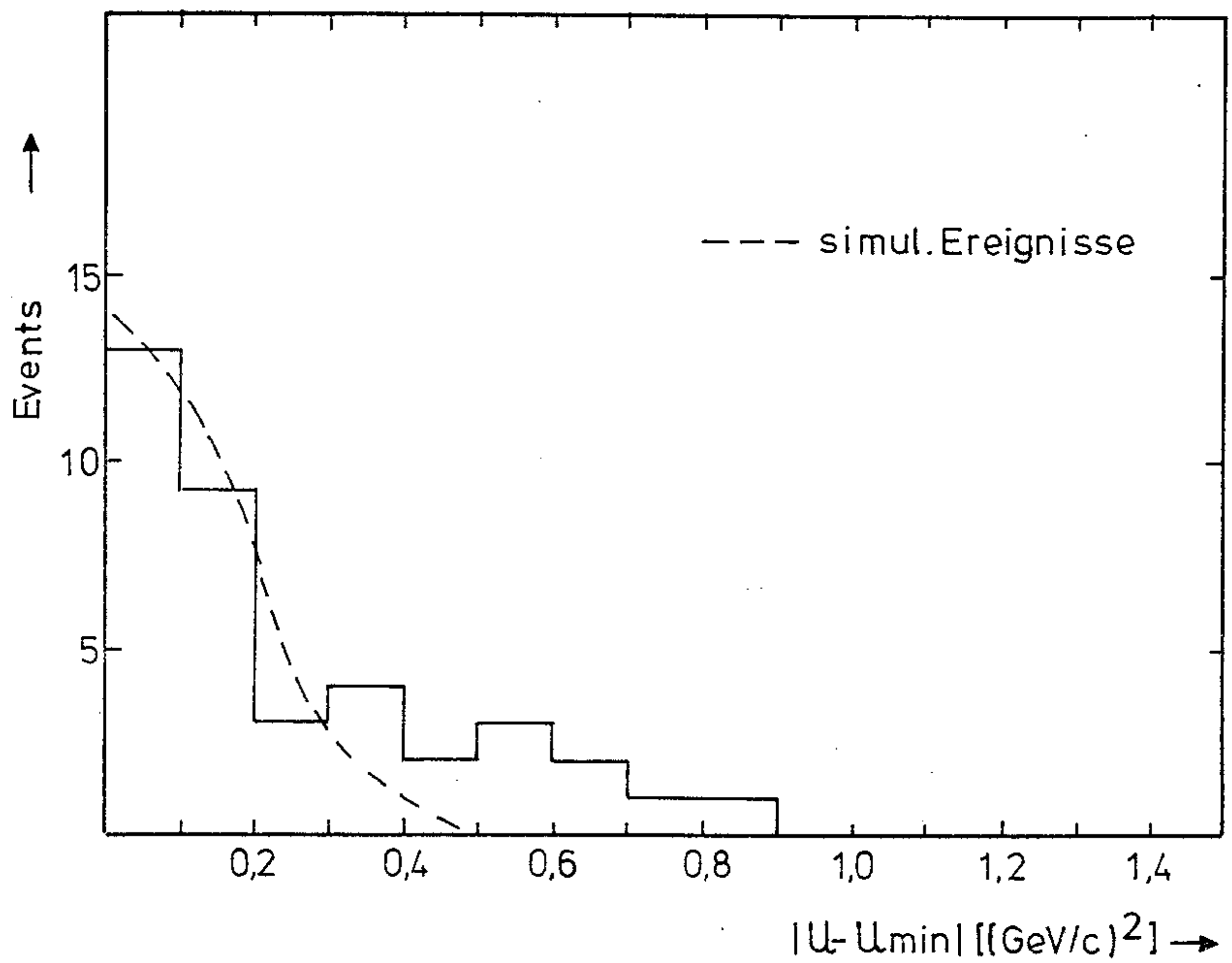

simul. Ereignisse
Events
15
10
5
0,2
0,4
0,6
0,8
1,0
1,2
1,4
|u-umin| [(GeV/c)2]

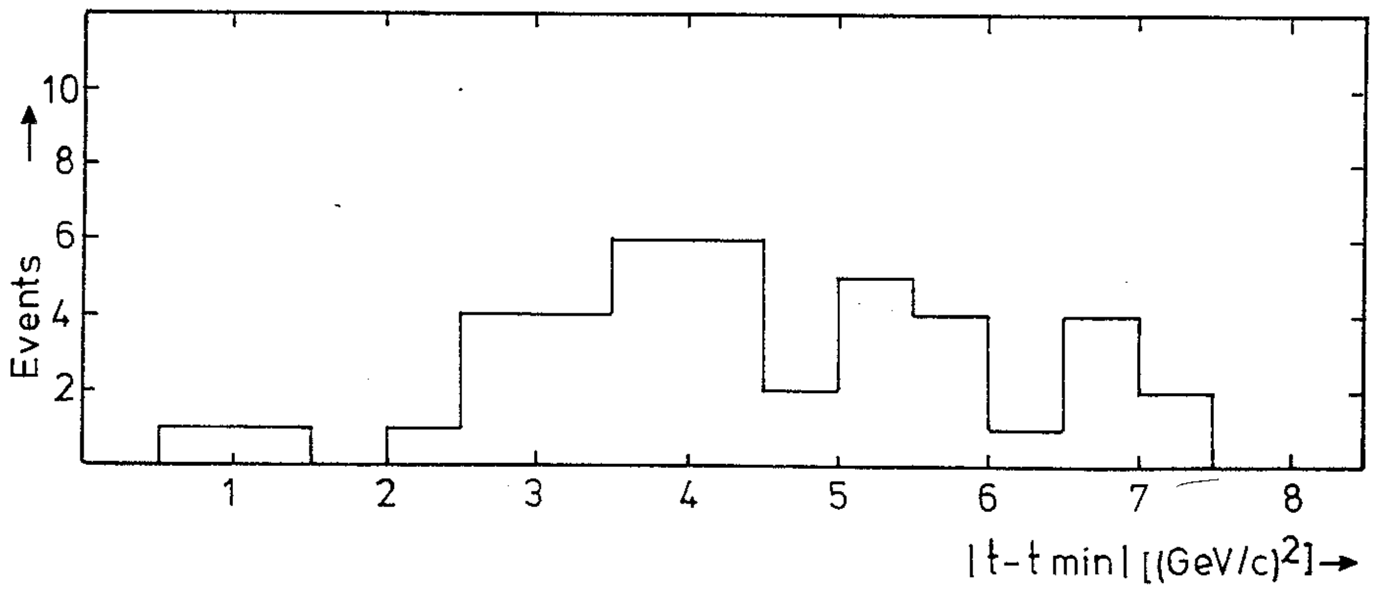

Events
10
8
6
4
2
1
2
3
4
5
6
7
8
|t-t min| [(GeV/c)2]

Fig. 6

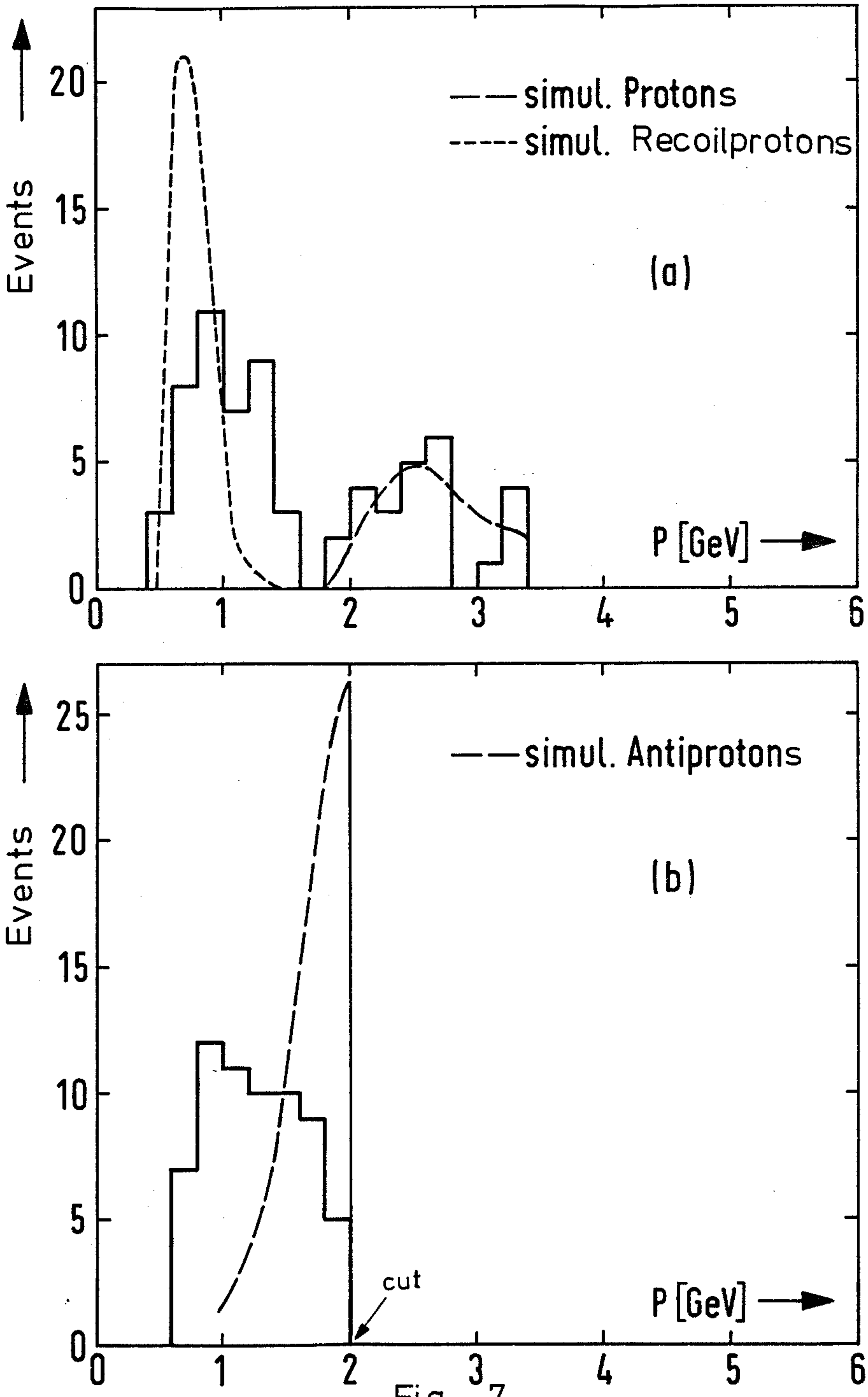

simul. Protons
simul. Recoilprotons
(a)
Events
P [GeV]
0
5
10
15
20
0
1
2
3
4
5
6
simul. Antiprotons
(b)
Events
P [GeV]
cut
0
5
10
15
20
25
0
1
2
3
4
5
6

Fig 7

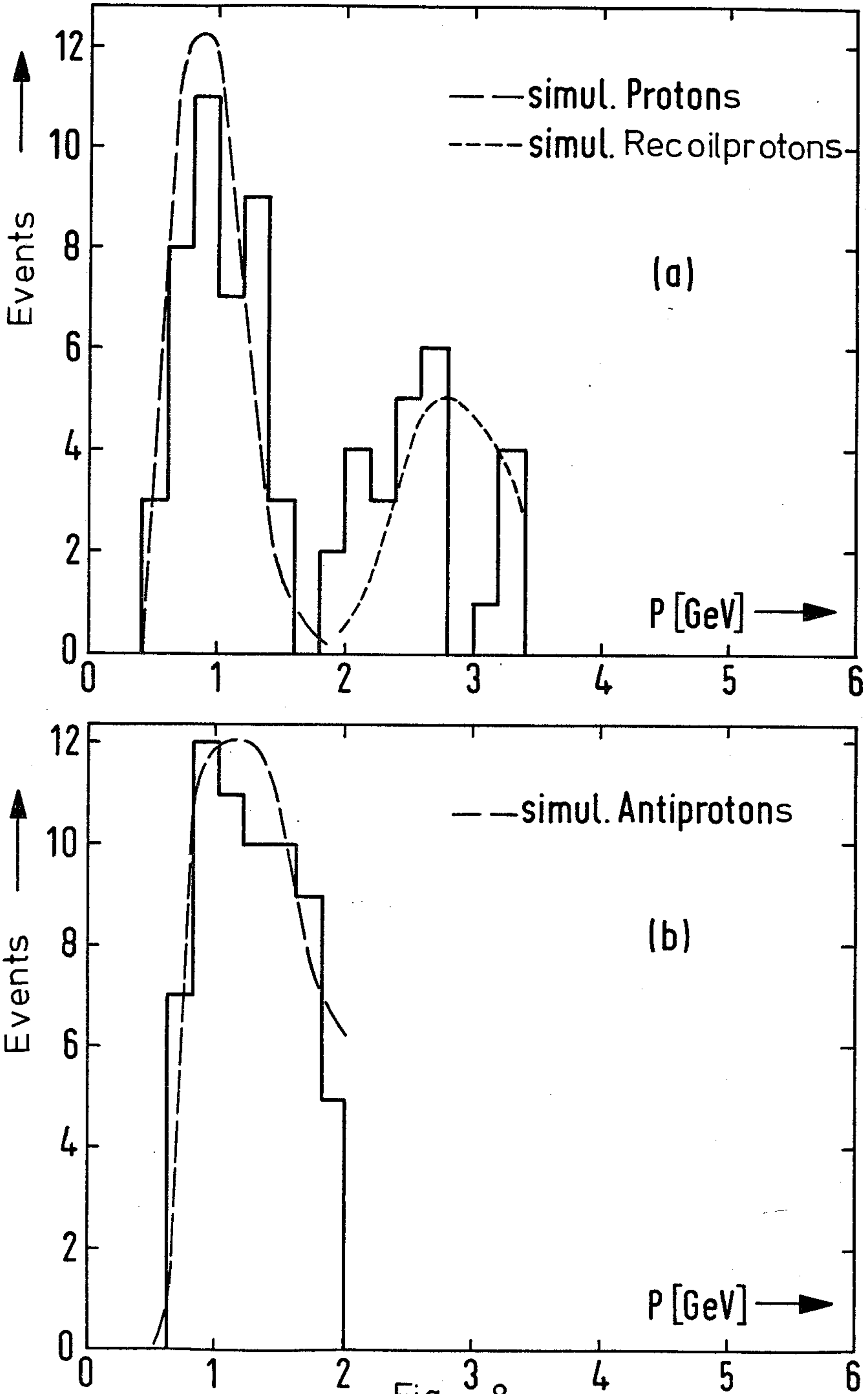

Events
12
10
8
6
4
2
0
simul. Protons
simul. Recoilprotons
(a)
P [GeV]
0
1
2
3
4
5
6
simul. Antiprotons
(b)

Fig. 8

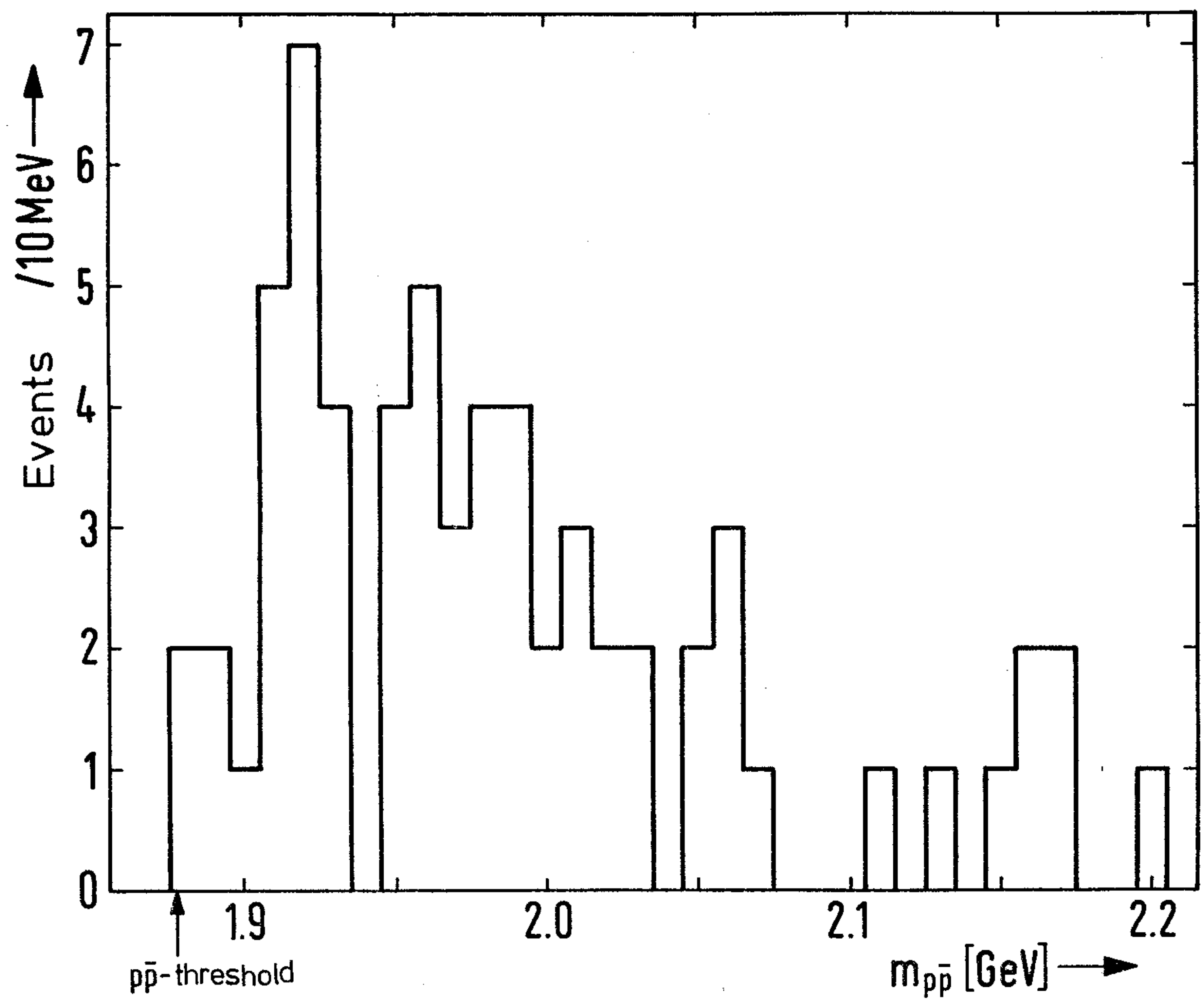

Fig. 9